Mechanics of Materials 124 (2018) 26–32

Contents lists available at ScienceDirect

Mechanics of Materials

journal homepage: www.elsevier.com/locate/mechmat

Research paper

Strength failure criteria analysis for a flax fibre reinforced composite

Rachel Koh*,[a], Bo Madsen[b]

[a] Department of Mechanical Engineering, Lafayette College, United States
[b] Section of Composites and Materials Mechanics, Department of Wind Energy, Technical University of Denmark, Denmark

ARTICLE INFO

Keywords:
Flax
Failure criteria
Natural fibre composite

ABSTRACT

Natural fibre composites are being utilized increasingly in high-performance, structurally demanding applications, in part because of their material properties and in part because they are a more sustainable choice compared to other engineering materials. However, there is a current lack in understanding of best practices for strength modelling of natural fibre composites. This study aims to understand how well common failure criteria predict strength in multidirectional flax fibre composite laminates. Four failure criteria are compared to experimental data from tension and compression tests of flax composite laminates with five different layups. Parametric optimization is performed on each criterion in order to determine the optimal strength, stiffness, and interaction parameters. In conclusion, the Hashin and Puck failure theories are recommended because they have the smallest error compared to experimental data. Values for parallel-to-fibre shear strength are also presented, and they are found to be comparable to the shear strength of conventional glass fibre composites with similar matrix materials.

1. Introduction

Natural fibre composites are being utilized increasingly in high-performance, structurally demanding applications, in part because of their material properties and in part because they are a more sustainable choice than other engineering materials, such as mined or petroleum-based materials. Natural fibre composites have excellent specific strength and stiffness properties, meaning that they are very strong and very stiff, but also lightweight (Shah, 2014). This has made natural fibres especially attractive for multi-megawatt wind turbine blades because of how critical a blades mass is for blade and turbine design. In addition, through natural fibre composites, the potential exists for blades to be carbon neutral and based on renewable resources.

The use of natural fibres in composite materials has been studied extensively (Saheb and Jyoti, 1999; Mohanty et al., 2002; Faruk et al., 2012). From 2000 to 2007, over 500 patents were filed and over 150 articles were written on the subject of natural fibre composites (Faruk et al., 2012). However, the strength and failure properties of these composites have been less studied. In particular, the field lacks a framework for strength of multidirectional natural fibre composites, and strength of the composites under complex stress states.

When modelling a material in a finite element software, it is common to use failure criteria to predict failure of the material when exposed to complex loading conditions. Failure criteria consider all stress tensor components to predict failure in combined loading scenarios, including those that result from multidirectional composite laminates. At present, however, in the industry for conventional glass and carbon fibre composites, there is disagreement on the best practice for the treatment of composite failure (Sun et al., 1996). In such fibre-reinforced composites, it is well known that fibres follow a random distribution pattern within the matrix (Wang et al., 2016), and that the resulting composite mechanical properties are also a randomly distributed (Mahesh et al., 2002). In the literature, there are numerous criteria which have been proposed for strength modelling in composite materials. These include the Tsai–Hill criterion (Hill, 1948), the Tsai–Wu criterion (Tsai and Wu, 1971), the Hashin criterion (Hashin, 1980), and the Puck criterion (Puck and Schurmann, 1998).

The use of parametric optimization in combination with failure theories has been used previously (Koh and Clouston, 2017) to report shear strength and interaction parameters of laminated wood, which are difficult to determine experimentally and not widely reported in the literature. A similar method has also been used to present best-fit failure theories for wood laminates (Koh, 2016), and a comparison has been made to demonstrate the difference between using parameters from the literature and parameters from the optimization algorithm. The use of parametric optimization in combination with failure theories allows a framework for understanding the strength of all multidirectional materials, and thus is also well suited for composite laminates.

This study aims to understand how well common failure criteria predict strength in multidirectional flax fibre composite laminates. Four

* Corresponding author.
E-mail address: kohr@lafayette.edu (R. Koh).

https://doi.org/10.1016/j.mechmat.2018.05.005
Received 29 December 2017; Received in revised form 28 April 2018; Accepted 22 May 2018
Available online 24 May 2018

failure criteria are compared to experimental data from tension and compression tests of flax composite laminates with five different layups. Parametric optimization is performed on each criterion in order to determine the optimal strength, stiffness, and interaction parameters. The study concludes with remarks on which failure theories are best suited for computational modelling of multidirectional flax fibre composites, and gives recommendations for best practices.

2. Methods

2.1. Materials

Unidirectional (UD) and multidirectional (MD) composite laminates were manufactured using vacuum infusion. The fibre component is a 2-ply, non-crimp, biaxial flax yarn fabric from Bcomp Ltd., Switzerland, called Amplitex 5008, with an area weight of 350 g/m^2. Its yarn orientation is nominally $+/-45^\circ$ in the machine direction of the fabric, but was measured in the present study to be $+51/-52^\circ$. The polyester stitches that hold the two plies in the fabric together were carefully removed with tweezers so that the plies could be re-oriented for making a UD laminate. In the case of the MD laminates, the stitches were also removed for consistency. The applied layup for the composites consisted of 4 fabric sheets placed on top of each other, resulting in a fibre orientation of 0° for the UD laminate, and $+51/-52^\circ$ for the MD laminates. The matrix component is Huntsmans Araldite 1568 / Aradur 3489 epoxy resin, using a mix ratio of 100:28 parts by weight. The cure cycle is 19 h at 40 °C followed by 5 h at 75 °C. The resulting 8-ply (i.e. layup of 4 fabric sheets) laminates have planar dimensions of 400 × 400 mm (UD) and 470 × 670 mm (MD), and thickness of 2.4 mm (UD) and 2.8 mm (MD).

Composite density (ρ_c) was measured using Archimedes' principle, where 3 specimens measuring 25 × 25 mm were cut from each plate and weighed submerged in water. Volumetric composition of the composites (V_f, V_m, and V_p) was calculated using measured values of density and weight fraction (W_f), as demonstrated in Eqs. (1a)–(1c). Density of the flax fibres (ρ_f) was taken to be 1.540 g/cm^3 from a previous study (Madsen and Lilholt, 2003) and density of the cured epoxy matrix was measured to be 1.14 g/cm^3.

$$V_f = \left(\frac{\rho_c}{\rho_f}\right) * W_f \tag{1a}$$

$$V_m = \left(\frac{\rho_c}{\rho_m}\right) * (1 - W_f) \tag{1b}$$

$$V_p = 1 - V_f - V_m \tag{1c}$$

In order to get a representation of different fibre orientations, mechanical test specimens were cut from the laminates at different angles. UD specimens were cut at two angles, 0° and 90° from the UD laminate. MD specimens were cut at three angles, 0°, 15°, and 90° from the MD laminate. See Fig. 1 for a schematic drawing of the cut test specimens.

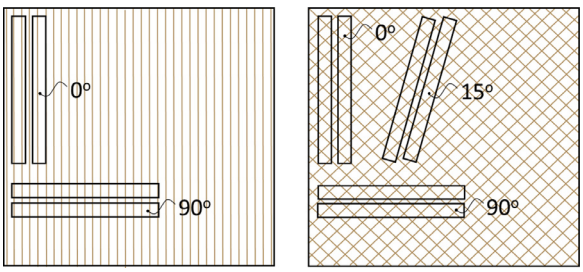

Fig. 1. Schematic drawing of the mechanical test specimens cut from the UD laminate (left) and MD laminate (right), giving specimens with five different fibre orientations.

The tensile test specimens had rectangular dimensions (width x length) of 15 × 250 mm (UD) and 25 × 250 mm (MD), gauge section lengths of 50 mm (UD and MD), and grip lengths of 50 mm (UD and MD), as per the tension testing standard IS0527-4 (Standard, 1997). Dogbone-shaped specimens were cut for compression tests with total dimensions of 19 × 136 mm (UD and MD), grip lengths of 51 mm with tapered tabs, and gauge sections of 15 × 14 mm.

2.2. Experimental methods

Static tensile tests were performed on an Instron test machine with a crosshead speed of 1 mm/min, grip capacity of 100 kN and loadcell capacity of 20 kN. Tests were done at room temperature. Strain was measured with two extensometers, centred on either side of the test specimen. Ultimate strength was determined as the recorded maximum stress, and stiffness was determined in the strain range of 0.05% to 0.25%. Static compression tests were performed using a mechanical combined loading fixture (Bech et al., 2011), which applies a fixed ratio of end-to-shear loading. This fixture has proven to yield repeatable results and acceptable failure modes in tests with glass and carbon fibre composites (Bech et al., 2011). The fixture was mounted on an Instron test machine. Strain gauges were used on either side of the test specimen. Specimens were strained to failure at a crosshead speed of 1 mm/min. Ultimate strength was determined as the recorded maximum stress, and stiffness was determined in the strain range of 0.05%–0.25%.

Prior to mechanical testing, the fibre angles of the test specimens were measured using a Fast Fourier Transform (FFT) image analysis procedure, as shown in Fig. 2. The term 'fibre angle' is used to refer to the angle of the yarn in the specimen relative to the testing direction, and as such it does not account for the twist direction of the fibres in the yarn (Madsen et al., 2007). First, photographs of specimens were taken on a light table using a Sony A7R II digital camera (Fig. 2, left). It was possible to capture all 8 plies at once by using front-light from the light table, with individual plies being indistinguishable from one another. Then, MATLAB' s FFT algorithm was used to transform the photograph into a frequency domain image (Fig. 2, middle). The reference direction of the specimen is defined by the lengthwise specimen edge. In addition to the detected main fibre direction frequencies, smaller contributions from other frequencies were also detected in each image (Fig. 2, right). These frequencies were filtered out using a high-pass filter. Finally, the mean fibre angles were taken by averaging the two clusters that passed through the filter.

2.3. Composite laminate analysis

From experimental data, global stresses and strains were transformed into lamina stresses and strains following the assumptions of Classical Lamination Theory (CLT), as shown in Fig. 3. It is these lamina-level stresses and strains that are employed in failure criteria. The global coordinate system is defined by (σ_x, ϵ_x) where x is the testing direction. The lamina coordinate system is defined by (σ_1, ϵ_1) representing the parallel-to-fibre direction and (σ_2, ϵ_2) representing the perpendicular-to-fibre direction.

2.4. Failure criteria

Failure criteria are used in computational modelling of composite structures to describe *when a material will fail under multiple and simultaneous types of stresses* (e.g. axial, transverse, and shear). The failure theories presented herein are all simplified into plane stress formulations, as is employed in the analysis of plates or shells.

There is considerable disagreement in the literature about what the correct definition of failure is for composite laminates. Herein, *ultimate strength is used to define failure* because this is a clearly defined point of the measured stress-strain curves. Different definitions of failure could,

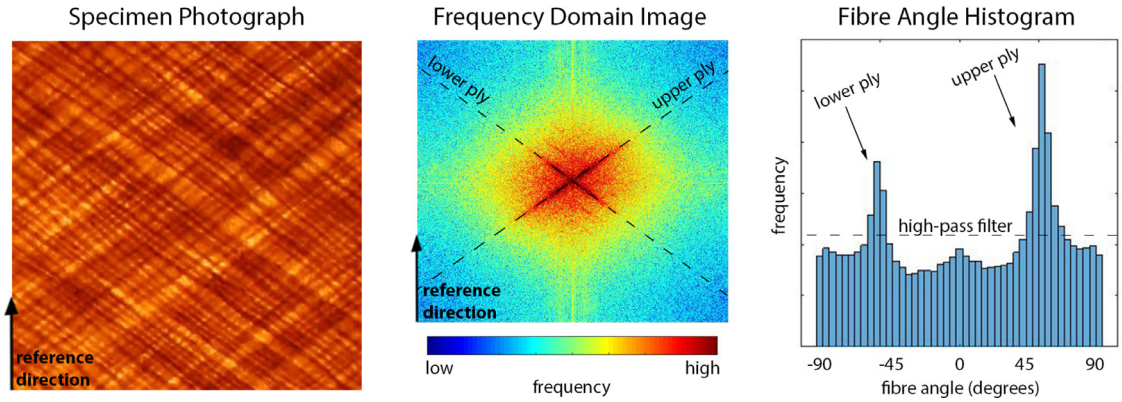

Fig. 2. Image analysis procedure to measure fibre angles in test specimens by using Fast Fourier Transform (FFT). *Left:* Example of specimen photograph of a MD specimen with fibre angles of $+51/-52$. *Centre:* Scaled and centred FFT frequency domain image. *Right:* Histogram showing the fibre angle distribution detected by FFT.

however, straightforwardly be implemented in the presented optimization methodology. Next follows descriptions of the failure criteria used in the present study.

2.4.1. Tsai–Hill Criterion

Eq. (2) represents the in-plane formulation of the Tsai–Hill failure criterion (Tsai, 1968; Hill, 1948). The Tsai–Hill theory is used widely in composite laminate analysis. While its clear disadvantage is that it does not consider tensile and compressive behaviour separately, it is a good basis for comparison between other criteria because of its widespread and historical use. The parameter σ is used to denote stress, while S is used to denote strength. Subscripts 1 and 2 refer to parallel-to-fibre and perpendicular-to-fibre directions, respectively, and the combined subscript 12 denotes shear.

$$\left(\frac{\sigma_1}{S_1}\right)^2 + \left(\frac{\sigma_2}{S_2}\right)^2 + \left(\frac{\sigma_{12}}{S_{12}}\right)^2 - \left(\frac{\sigma_1\sigma_2}{S_1^2}\right) = 1 \tag{2}$$

2.4.2. Tsai–Wu Criterion

Eqs. (3a) and (3b) represent the in-plane formulation of the Tsai–Wu failure criterion (Tsai and Wu, 1971). The Tsai–Wu theory is also used widely, especially in finite element modelling of composites. It is easy to implement, like the Tsai–Hill criterion, but it offers the advantage of considering tensile and compressive strengths separately. In Eq. (3), subscripts T and C refer to tension and compression, respectively. The parameter f_{12} accounts for the interaction between the normal stresses σ_1 and σ_2. In this study, the optimization bounds for f_{12} are determined by a stability condition which requires the surface to converge (Clouston et al., 1998).

$$f_1\sigma_1 + f_2\sigma_2 + f_{11}\sigma_1^2 + f_{22}\sigma_2^2 + f_{66}\sigma_{12}^2 + 2f_{12}\sigma_1\sigma_2 = 1 \tag{3a}$$

$$f_1 = \frac{1}{S_{1T}} - \frac{1}{S_{1C}};\ f_2 = \frac{1}{S_{2T}} - \frac{1}{S_{2C}};\ f_{11} = \frac{1}{S_{1T}S_{1C}};\ f_{22} = \frac{1}{S_{2T}S_{2C}};\ f_{66} = \frac{1}{S_{12}^2} \tag{3b}$$

2.4.3. Hashin criterion

The Hashin failure criterion (Hashin, 1980) (Eqs. (4a)–(4d)) presents a semi-empirical approach, to address the problem that the different phases of a composite material (typically fibre and matrix) cause them to fail in different modes. Prior criteria had only allowed these modes to be represented by variation in the interaction parameters. Hashin defines four modes by which the composite could fail and considers the stress state under which each would occur, resulting in a piecewise failure surface. Several updates have been proposed to the original yield theory to account for phenomenological differences in the behaviour of different materials (e.g. the Sun criterion for matrix compression (Sun and Tao, 1998)). In the present study, Hashin's original theory is used.

1. Tensile Fiber Mode

$$\left(\frac{\sigma_1}{S_{1T}}\right)^2 + \left(\frac{\sigma_{12}}{S_{12}}\right)^2 = 1;\quad \sigma_1 > 0 \tag{4a}$$

2. Fiber Compressive Mode

$$\sigma_1 = -S_{1C};\quad \sigma_1 < 0 \tag{4b}$$

3. Tensile Matrix Mode

$$\left(\frac{\sigma_2}{S_{2T}}\right)^2 + \left(\frac{\sigma_{12}}{S_{12}}\right)^2 = 1;\quad \sigma_2 > 0 \tag{4c}$$

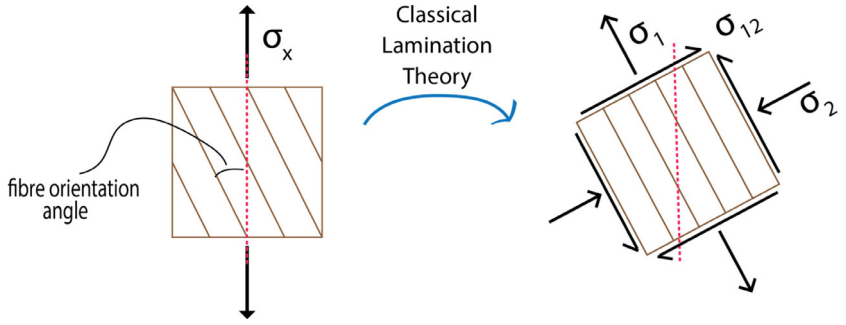

Fig. 3. Classical Lamination Theory is used to convert global stresses and strains (in the testing direction) into lamina stresses and strains (in the fibre direction).

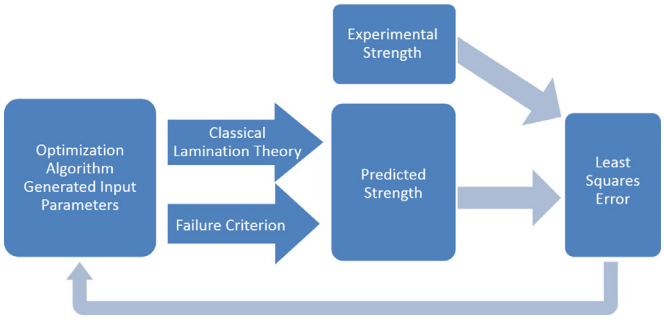

Fig. 4. Schematic of parametric optimization procedure applied to fit failure criteria to the experimental strength data.

4. Compressive Matrix Mode

$$\left(\frac{\sigma_2}{S_{21}}\right)^2 + \left[\left(\frac{S_{2C}}{2S_{21}}\right)^2 - 1\right]\frac{\sigma_2}{S_{2C}} + \left(\frac{\sigma_{12}}{S_{12}}\right)^2 = 1; \quad \sigma_2 < 0 \tag{4d}$$

2.4.4. Puck criterion

The Puck failure criterion (Eqs. (5a)–(5e)) (Puck and Schurmann, 1998) was chosen because of its success in the World-Wide Failure Exercise, which assessed 13 different failure theories in 125 different cases (Hinton et al., 2002). Puck' s theory did particularly well in the category of cases which assessed ultimate strengths of multi-directional composite laminates. Puck' s approach distinguishes between two main failure types: Fibre Failure (FF) and Inter-Fibre Fracture (IFF). The FF failure type is subcategorized into tension and compression modes, while IFF failure type is subcategorized into Modes A, B, and C, which depend upon the ratio of transverse (σ_2) to shear (σ_{12} or σ_{21}) stress. Furthermore, Puck' s theory is the only one considered here which includes a degradation model, describing laminate behaviour after crack initiation and allowing a distinction between initial and final failure. However, in order to be consistent with the other failure theories, this study does not distinguish between initial failure and final failure. Instead, only final failure is considered.

In the Puck criterion, $\epsilon_1 T$ and $\epsilon_1 C$ are used to represent *ultimate* strain in tension and compression, respectively, and ϵ_1 is the *current* strain. γ_{12} is shear strain, which is assumed to be equal to zero on tests of unidirectional laminates. The parameter ν_{f12} is the Poissons ratio for fibres, and $m_{\sigma f}$ is a mean stress magnification factor for fibres in the transverse direction and is assumed to be equal to 1 for the tests of unidirectional laminates. The parameter $p_{\perp\parallel}^{(-)}$ is the slope of the (σ_1, σ_{12}) failure curve when $\sigma_1 <= 0$, $p_{\perp\parallel}^{(+)}$ is the slope of the (σ_1, σ_{12}) failure curve when $\sigma_1 > 0$, and $p_{\perp\perp}^{(-)}$ is the slope of the (σ_1, σ_{21}) failure curve when $\sigma_1 <= 0$. The parameter σ_{1D} is a stress value for linear degradation.

1. FF Tension

$$\frac{1}{\epsilon_{1T}}\left(\epsilon_1 + \frac{\nu_{f12}}{E_{f1}} m_{\sigma f}\sigma_2\right) = 1 \tag{5a}$$

2. FF Compression

$$\frac{1}{\epsilon_{1C}}\left|\left(\epsilon_1 + \frac{\nu_{f12}}{E_{f1}} m_{\sigma f}\sigma_2\right)\right| = 1 - (10\gamma_{21})^2 \tag{5b}$$

3. IFF Mode A

$$\sqrt{\left(\frac{\sigma_{12}}{S_{21}}\right)^2 + \left(1 - p_{\perp\parallel}^{(+)}\frac{S_{2T}}{S_{21}}\right)^2\left(\frac{\sigma_2}{S_{2T}}\right)^2} + p_{\perp\parallel}^{(+)}\frac{\sigma_2}{S_{21}} = 1 - \left|\frac{\sigma_1}{\sigma_{1D}}\right| \tag{5c}$$

4. IFF Mode B

$$\frac{1}{S_{21}}\left(\sqrt{\sigma_{21}^2 + \left(p_{\perp\parallel}^{(-)}\sigma_2\right)^2} + p_{\perp\parallel}^{(-)}\sigma_2\right) = 1 - \left|\frac{\sigma_1}{\sigma_{1D}}\right| \tag{5d}$$

5. IFF Mode C

$$\left[\left(\frac{\sigma_{21}}{2(1 + p_{\perp\perp}^{(-)})S_{21}}\right)^2 + \left(\frac{\sigma_2}{S_{2C}}\right)^2\right]\frac{S_{2C}}{-\sigma_2} = 1 - \left|\frac{\sigma_1}{\sigma_{1D}}\right| \tag{5e}$$

2.5. Optimization

The FMINCON optimization solver in MATLAB was used to optimize the various strength, strain and interaction parameters of the failure criteria equations with respect to the experimental data. A schematic for the parametric optimization procedure is depicted in Fig. 4. First, the stress tensors are calculated from the experimental data using CLT, with the measured fibre orientations in the composite laminates. During this step, the strength properties were corrected using the rule of mixtures to account for any difference in fibre volume fractions between UD and MD laminates. Next, the strength and other parameters are substituted into the failure criterion which is solved for the predicted stress tensor. The fitness function minimizes the least squares error between the predicted failure and the experimental failure for each of the analysed fibre orientations.

3. Results

3.1. Composite properties

As shown in Table 1, the UD and MD composite laminates were fabricated with fibre volume contents of 37% and 31%, respectively. The higher fibre content in the UD laminate is expected due to the better packing ability of the fibre yarns when the two plies of the fabrics are aligned with each other. The porosity content for both composites is below 1% indicating good materials quality. Table 1 presents also the measured fibre angles of the test specimens. For the two UD test specimens, U1 and U2, the fibre angles are measured to be 0 and 87 degrees, respectively, which demonstrates that the approach of re-

Table 1
Physical properties of the manufactured flax composite laminates.

Composite laminate	Density (g/cm^3)	Fibre volume content, V_f (%)	Porosity, V_p (%)	Test specimen	Fibre angle (°)	
					Mean	SD
Unidirectional (UD)	1.28	37	0.7	U1	0	1.0
				U2	87	0.2
Multidirectional (MD)	1.26	31	0.7	M1	+51/−52	1.4/0.4
				M2	+36/−66	1.9/0.3
				M3	+38/−38	1.2/1.3

Table 2
Tensile and compression properties of the unidirectional and multidirectional flax composite laminates.

Tensile specimen	Fibre angle (°)	Tensile properties				
		No. of specimens	Stiffness (GPa)		Strength (MPa)	
			Mean	SD	Mean	SD
U1	0	10	20.3	1.5	269	27
U2	87	3	3.6	0.2	21	1
M1	+51/−52	8	4.5	0.1	45	1
M2	+36/−66	10	5.0	0.1	45	1
M3	+38/−38	6	7.5	0.3	109	3
Compression specimen	Fibre angle (°)	Compression properties				
		No. of specimens	Stiffness (GPa)		Strength (MPa)	
			Mean	SD	Mean	SD
U1	0	3	16.2	0.4	−110	0
U2	87	2	4.5	0.6	−76	5
M1	+51/−52	3	4.1	0.2	−87	2
M2	+36/−66	–	–	–	–	–
M3	+38/−38	3	5.6	0.2	−90	2

orienting the two plies in the fabric was successful. For the three MD test specimens, M1, M2 and M3, the fibre angles are measured to be +51/−52°, +36/−66° and +38/−38°, respectively. These angles are almost identical to the expected values based on the cutting angles of the specimens (see Fig. 1), i.e. for M2: 51° − 15° = 36°, − 52° − 15° = −67°, and for M3: 90° − 52° = 38°, 51° − 90° = −39°.

Tension and compression tests were performed on the test specimens from the UD and MD composite laminates. The resulting stiffnesses and strengths are reported in Table 2. The variation in number of specimens per fibre orientation is a result of optimizing the cut plan of the laminates, and prioritizing fibre orientations in which fibre failure is expected. Failure modes governed by fibre failure are known to have more variation compared to composite failure modes governed by matrix failure (Gibson, 2007). Additionally, a smaller number of specimens were tested in compression because of the greater complexity in performing these tests. The results presented in Table 2 for tensile properties are consistent with Madsen and Lilholt (2003) and Madsen and Gamstedt (2013) who reviewed the subject, presenting results from several studies of natural fibre composites. For the UD laminate, the U1 tensile specimen has a stiffness of 20 GPa. By using a simple rule-of-mixtures relationship, the effective stiffness of the flax fibres can be back-calculated to be 48 GPa, which is a typical stiffness value for flax fibres in composites (Madsen et al., 2009). Compression properties are less studied and there is limited availability of data for which to compare with the results in the present paper. However, previous research has shown that compressive strength tends to be similar but somewhat less than tensile strength (Bos, 2004). This trend is consistent with the findings for the U1 and M3 test specimens, where fibre failures were observed. In cases where matrix failure was observed (U2 and M1), compression strength is higher than tensile strength. Compressive stiffness is similar to tensile stiffness across all specimens.

For the UD laminate, the tensile strength in the 0° direction (U1 specimens) was corrected to be 235 MPa (instead of 269 MPa) using the rule of mixtures, to account for the lower fibre content in the MD laminate of 31% (instead of 37%). This correction was made to bring UD and MD specimens to the same volume fraction. The tensile strength in the 90° direction (U2 specimens) was not corrected, due to the known low sensitivity of the fibre content on strength in this direction (Madsen and Lilholt, 2003). Due to the lack of widely accepted analytical models for compression properties of composites, it was decided not to correct the compression strength values of the UD laminate.

Table 3
Optimal model parameters for Tsai–Hill, Tsai–Wu, Hashin and Puck failure criteria, and the related mean errors (fitness).

(a) Tension, compression, and shear strength parameters.

Failure criterion	Parameter					
	S_{1T} (MPa)	S_{1C} (MPa)	S_{2T} (MPa)	S_{2C} (MPa)	S_{12} (MPa)	Mean error (%)
Tsai–Hill	110	−110	23	−23	58	19
Tsai–Wu	112	−42	21	−79	37	15
Hashin	240	−112	20	−97	37	7
Puck	–	–	21	−77	43	6

(b) Additional strength, strain, and interaction parameters.

Failure criterion	Parameter	Value
Tsai Wu	$f_{12,\,T}$ (MPa^{-2})	0
	$f_{12,\,C}$ (MPa^{-2})	0
Hashin	S_{21} (MPa)	−87
Puck	ϵ_{1T}	2.0
	ϵ_{1C}	−3.2
	$p_{\perp\parallel}^{(+)}$	0.42
	$p_{\perp\parallel}^{(-)}$	−1.57
	$p_{\perp\perp}^{(-)}$	−0.50

3.2. Failure criteria

The parameters of the four failure criteria were optimized by using a minimization algorithm to fit the equations of the criteria to the experimental data of the UD and MD specimens. The generated optimal parameter values, along with the mean error (fitness), are reported in Table 3.

Fig. 5 depicts plots of each failure theory in $\sigma_1 - \sigma_2$ space. This is a common representation of failure criteria. However, since the $\sigma_1 - \sigma_2$ space does not depict shear stress, it does not capture how well the theories predict failure of MD composites. It is therefore most useful to notice how well the theories fit failure of UD composites. It is clear from the plots that the Hashin and Puck theories fit the UD specimens best, while the Tsai–Hill and Tsai–Wu theories are quite far off. Fig. 6 depicts plots of the theories in $\sigma_2 - \sigma_{12}$ space. It is often useful to look at failure criteria in this plane because it constitutes matrix (or inter-fibre) failures. This view better depicts the fit of each theory to the failure of the three MD specimens, together with the U2 specimens. The Tsai–Wu, Hashin, and Puck theories all perform well in this space.

The Tsai–Hill theory gives the highest error at 19.9% and is clearly not a good fit to experimental data because of its neglect to consider tensile and compressive properties separately. It was chosen for this study because of its use historically and in the industry, and chosen as a baseline from which to compare other theories. As seen in Fig. 5, much of the error of the Tsai–Hill failure criterion comes from parallel-to-fibre tension and perpendicular-to-fibre compression. Matrix failure is more closely predicted, as seen in Fig. 6, but strength is overestimated for all cases where $\sigma_2 > 0$, and underestimated in all cases where $\sigma_2 < 0$, highlighting the major drawback of the Tsai–Hill theory, which is that it fails to consider tensile and compressive strength separately.

The Tsai–Wu theory is an improvement compared to Tsai–Hill because of its consideration for tensile and compressive properties separately, but the Tsai–Wu theory is limited by its ellipsoidal formulation, and thus gives very conservative strength values in tension and compression parallel-to-fibres. While with the optimal parameters, it predicts matrix failure well (Fig. 6), it far under-predicts the fibre failures (Fig. 5), leading to a high mean error of 15%. It should also be noted that the optimal strength parameters found for this theory (see Table 3) are far less than strengths reported in the literature for typical natural fibre composites. Thus, importantly, if this theory was implemented

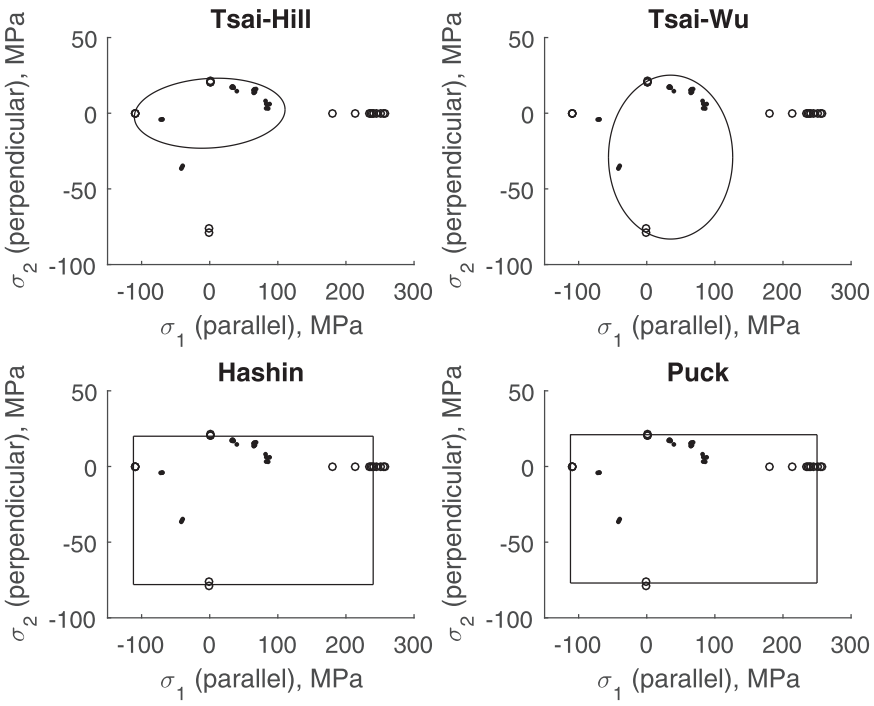

Fig. 5. Tsai–Hill, Tsai–Wu, Hashin, and Puck failure criteria in $\sigma_1 - \sigma_2$ space with $\sigma_{12} = 0$. Experimental data are shown with UD specimens marked by open dots and MD specimens marked by filled dots.

using parameters from the literature (S_{1T}, S_{1C} etc.), the Tsai–Wu criterion would far overestimate composite strength in cases of matrix failure. Finally, it can be noted that the Tsai–Wu theory uses interaction parameters, $f_{12,\ T}$ and $f_{12,\ C}$, which are difficult to determine experimentally. Within the optimization bounds (determined by the stability criterion previously mentioned), $f_{12,\ T}$ and $f_{12,\ C}$ were found to have negligible effect on the fit of the surface; therefore it is recommended to use $f_{12,T} = f_{12,C} = 0$.

The Hashin theory demonstrates a relatively low mean error of 7%, and it also demonstrates optimal strength parameters which align closely with what exists in the literature for typical natural fibre composites. The main disadvantage to the Hashin theory, as compared to Tsai–Hill or Tsai–Wu, is that it is of moderate complexity, requiring four piecewise equations which depend upon the fracture mode. Considering the use of four equations, though, it does not use interaction or other parameters, which are often difficult to determine experimentally; in this way it is still relative simple to implement.

The Puck theory shares several of the advantages of the Hashin

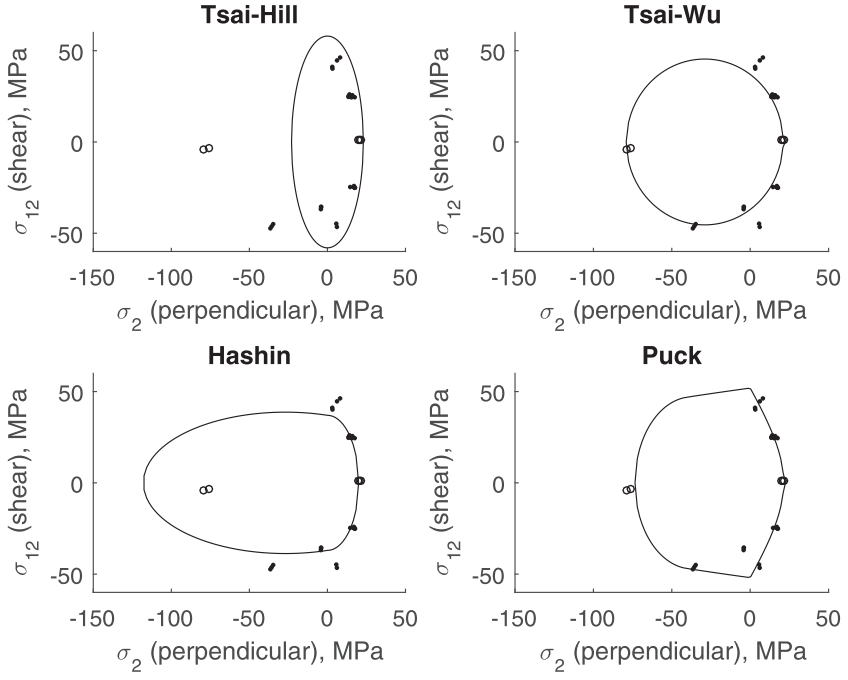

Fig. 6. Tsai–Hill, Tsai–Wu, Hashin, and Puck failure criteria plotted with experimental data in $\sigma_2 - \sigma_{12}$ space. Experimental data represents only samples which failed in this mode, i.e. U2, M1, M2, M3.

theory, and it has the lowest mean error of 6% among the presented four theories. The main disadvantage to the Puck theory is that it is of high complexity with five modes of failure and two parameters, $p^{(+)}$ and $p^{(-)}$, in addition to the strength and strain parameters. The parameters $p^{(+)}$ and $p^{(-)}$ define the slopes of the (σ_2, σ_{12}) failure curve for $\sigma_2 > 0$ and $\sigma_2 < 0$, respectively, and are determined empirically in practice. The Puck theory is the best fit for inter-fibre failures because it allows for three different modes of matrix failure, as opposed to the Hashin criterion which allows for two modes of matrix failure. Furthermore, the Puck theory includes a degradation model. While this model is not used herein, it is a good subject for further study and one of the reasons why the Puck criterion is recommended by Hinton et al., (2002) and Hinton et al. (2002).

In general, for strengths (and ultimate strains in the case of the Puck theory) of natural fibre composites, it is recommended to use the values associated with the Hashin and Puck failure theories because of their lower mean errors. The Tsai–Hill and Tsai–Wu theories substantially under-predict S_{1T} and S_{1C}. Conversely, the piecewise formulation of the Hashin and Puck theories allow for a more accurate assessment of strength and ultimate strain.

A further conclusion from the present study is the demonstrated advantage of using parametric optimization in combination with failure theories to report shear strength and interaction parameters, which are difficult to determine experimentally and not widely reported in the literature. There is a lack of reported shear strength data for natural fibre composites in the literature today, but it is well known that the matrix component drives the composite shear strength more than the fibre component because shear failures are inter-fibre failures (IFF). Therefore, it is expected that there will not be a significant difference between these composites and those fabricated from glass fibres with similar matrix materials. The values reported for shear strength of the flax fibre composites, in the range 36–49 MPa for the four failure theories, are consistent with the design values for glass fibre composites with similar matrix types (28–48 MPa), as recommended by the AIMS Fiberglass Structural Design Manual (LLC, 2017). The results indicate that, on the coupon testing scale, the natural fibre composites demonstrate mechanical behaviour which is consistent with other types of composites, and can be modelled using conventional computational methods. With the present set of parameters, it is now possible to design composite structures for ultimate strength from natural fibre composites.

4. Conclusions

A framework for evaluating the accuracy of failure criteria in comparison to experimental data, using tension and compression testing of multiaxial composite laminates, is presented. The Tsai–Hill, Tsai–Wu, Hashin, and Puck failure theories are compared to experimental data from tension and compression tests of flax composite laminates in five layups with varying fibre orientations. Each failure theory is coupled with a parametric optimization routine, and best-fit parameters are presented for each theory.

The Hashin and Puck theories have the lowest error compared to experimental data. Hashin' s theory offers the advantage of being more simple to implement, while Puck' s theory has the advantage of a degradation component, which allows for a plastic failure regime after yielding. The Tsai–Hill and Tsai–Wu theories, when fit to test data of multiaxial specimens, substantially under-predict uniaxial strengths S_1 (Tsai–Hill), S_{1T} and S_{1C} (Tsai–Wu). This also means that if these theories are used with common parameters reported in the literature, they would grossly overestimate the strength of multiaxial composite laminates.

Finally, the parametric optimization results lead to a measurement of parallel-to-fibre shear strength of flax laminate composites, a property which is difficult to determine experimentally and not widely reported in the literature.

References

Bech, J.I., Goutianos, S., Andersen, T.L., Torekov, R.K., Brondsted, P., 2011. A new static and fatigue compression test method for composites. strain. Int. J. Exp. Mech. 47, 21–28.

Bos, H., 2004. The Potential of Flax Fibres as Reinforcement for Composite Materials. Master's thesis, Technische Universiteit Eindhoven.

Clouston, P., Lam, F., Barrett, J.D., 1998. Interaction term of Tsai-Wu theory for laminated veneer. J. Mater. Civ. Eng. 10, 112–116.

Faruk, O., Bledzki, A.K., Fink, H.P., Sain, M., 2012. Biocomposites reinforced with natural fibers: 2000–2010. Prog. Polym. Sci. 37, 1552–1596.

Gibson, R.F., 2007. Principles of Composite Material Mechanics. CRC Press.

Hashin, Z., 1980. Failure criteria for unidirectional fiber composites. J. Appl. Mech. 47 (2), 329–334.

Hill, R., 1948. A theory of the yielding and plastic flow of anisotropic metals. Proc. R. Soc. Lond. A Math. Phys. Sci. 193, 281–297.

Hinton, M.J., Kaddour, A.S., Soden, P.D., 2002. A comparison of the predictive capabilities of current failure theories for composite laminates, judged against experimental evidence. Compos. Sci. Technol. 62 (12), 1725–1797.

Koh, R., 2016. Yield criteria assessment for angle-ply wood laminates in wind turbine blades. International Conference on Experimental Mechanics.

Koh, R.S., Clouston, P., 2017. In-plane shear properties of laminated wood from tension and compression tests of angle-ply laminates. J. Mater. Civ. Eng. 29, 11.

LLC, D. C. S., 2017. Design manual: Fiberglass grating and structural products. Tech. rep., Delta Composites LLC.

Madsen, B., Gamstedt, K., 2013. Wood versus plant fibers: similarities and differences in composite applications. Adv. Mater. Sci. Eng.

Madsen, B., Lilholt, H., 2003. Physical and mechanical properties of unidirectional plant fibre composites- an evaluation of the influence of porosity. Compos. Sci. Technol. 63 (9), 1265–1272.

Madsen, B., Thygesen, A., Lilholt, H., 2007. Plant fibre composites- porosity and volumetric interaction. Compos. Sci. Technol. 62, 1584–1600.

Madsen, B., Thygesen, A., Lilholt, H., 2009. Plant fibre composites- porosity and stiffness. Compos. Sci. Technol. 69, 1057–1069.

Mahesh, S., Phoenix, S.L., Beyerlein, I.J., 2002. Strength distribution and size effects for 2d and 3d composites with weibull fibers in an elastic matrix. Int. J. Fract. 115, 41–85.

Mohanty, A.K., Mizra, M., Drzal, L.T., 2002. Sustainable bio-composites from renewable resources: opportunities and challenges in the green materials world. J. Polym. Environ. 10 (1–2), 19–27.

Puck, A., Schurmann, H., 1998. Failure analysis of FRP laminates by means of physically based phenomenological models. Elsevier Compos. Sci. Technol. 1045–1067.

Saheb, D.N., Jyoti, P.J., 1999. Natural fiber polymer composites: a review. Adv. Polym. Tech. 18 (4), 351–363.

Shah, D., 2014. Natural fibre composites: comprehensive ashby-type materials selection charts. Mater. Des. 62, 21–31.

ISO Standard, 1997 Determination of tensile properties of plastics. Part 4: Test Conditions for Isotropic and Orthotropic Fibre-Reinforced Plastic Composites. International Organization for Standardization, Geneva, Switzerland, 527–4.

Sun, C., Quinn, B. J., Oplinger, D. W., 1996. Comparative evaluation of failure analysis methods for composite laminates. DOT/FAA/AR-95/109.

Sun, C., Tao, J., 1998. Prediction of failure envelopes and stress/strain behaviour of composite laminates. Compos. Sci. Technol 58 (7), 1125–1136.

Tsai, S., 1968. Strength theories of filament structures. In: Schwartz, R.T., Schwartz, H.S. (Eds.), Fundamental aspects of fiber reinforced plastic composites. Wiley Interscience, New York, pp. 3–11.

Tsai, S.W., Wu, E.M., 1971. A general theory of strength for anisotropic materials. J. Compos. Mater. 5, 58–80.

Wang, W., Dai, Y., Zhang, C., Gao, X., Zhao, M., 2016. Micromechanical modeling of fiber-reinforced composites with statistically equivalent random fiber distribution. Materials 9, 1–14.